International Journal of Air-Conditioning and Refrigeration Vol. 17, No. 2 (2009) 45~51

Analysis of Air Flow Rate through Subway Vent Shaft with Mechanical Ventilation System for Shape Change of Vent Shaft

Jung-Yup Kim†

Construction Quality Policy Department, Korea Institute of Construction Technology, Goyang, 411-712, Korea

(Received February 18, 2009; Revision received May 15, 2009; Accepted June 5, 2009)

Abstract

Three-dimensional numerical analyses of mechanical ventilation system in vent shaft of subway in operation are carried out in relation with the different air flow passage of vent shaft and two ventilation operation modes of push/pull. The ventilation characteristics of vent shaft with regard to the shape change are evaluated. And the air flow rate through the vent shaft by ventilation system is measured within subway in operation to assess the accuracy and applicability of the numerical analysis method. The decrease of air flow rate due to vent-shaft change are between 0.7 to 2.2% in the cases examined.

Key words: Subway ventilation, Vent shaft, Fan, Numerical analysis, Field experiment

1. Introduction

As traffic tends to increase drastically in line with growing industrialization and urbanization, the subway, with the benefit of superior punctuality and speed, has become the main transportation system in Korea as well as in other major countries. But, shaped as semi-closed tunnel, the subway is inevitably vulnerable to the fire, poor IAQ and thermal discomfort. So, it's strongly recommended to develop the technology for improving subway safety and environment.

Then, in the process of growth, development and extension of the urban area, the new roads are often designed on top of vent shaft of subway in operation as shown in Fig. 1. To accommodate the road construction, the vent shaft should be changed to outside of the new roadway and the geometry of air flow passage in vent shaft will accordingly be changed to other form. It will affect the ventilation system of vent shaft in which the blowers take outside air into subway tunnel or discharge the indoor air out of tunnel. The change of flow passage may increase the total flow drag while decreasing the flow rate for ventilation and smoke control in fire emergency. Thus, it's necessary to develop the construction method which will prevent the air flow rate through the vent shaft from being decreased.

In Seoul, the construction of "S"-Newtown has been planned, which caused one of mechanical vent shafts in "B"-subway line to be changed to outside the roadway. In a bid to conserve the environment of subway tunnel, it's needed to investigate to identify how the shape change of vent shaft affects the ventilation performance of vent shaft.

So far, a design of subway ventilation systems has been conducted mainly through the one-dimensional analysis method such as that in Subway Environmental Simulation[1], which are based on the simplified theory of flow analysis[2-3] and the

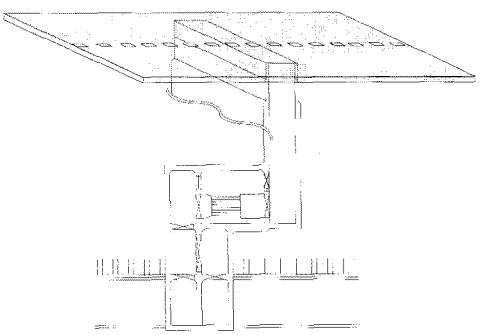

Fig. 1. New road designed on top of vent shaft.

†Corresponding author. Tel.: +82 31 369 0506, Fax.: +82 31 369 0540
E-mail address: jykim1@kict.re.kr

result of experimental studies[4]. While these one-dimensional analysis based methods are suitable for the design of subway ventilation systems in relation to the whole subway environment, these methods may not give the detailed and precise information needed to deal with the problems such as shape change of the vent shaft in subway. Recently, there has been significant development in three-dimensional numerical flow analysis technology and many applications aimed to analyze the air flow in subway tunnel have been presented [5-7].

In this study, in an attempt to examine the effect of vent-shaft changes, a three-dimensional numerical analyses of mechanical ventilation system in vent shaft of subway were carried out in relation with the different air flow passage of vent shaft and two ventilation operation modes of push/pull. And the air flow rate through the vent shaft in ventilation system was measured in subway to assess the accuracy and applicability of the numerical analysis method.

2. Analysis procedure

A schematic diagram of the vent shaft is shown in Fig. 2. Vent shaft is 33 m deep from the ground surface to tunnel, 2.5 m wide and 28.8 m long. Ventilation room is located in the middle to the vent shaft. After the work for shape-change, the air flow passage spins about 90 degree from above view. A 3D-diagrammatic view of the vent shaft before and after shape-change construction is shown in Fig. 3.

The fan in ventilation room is shown in Fig. 4. Total of 4 fans are installed and two set of fans (fan 1 and fan 3 / fan 2 and fan 4) operate in turn. There are 12 vents for air flow, which link the outside and ventilation room. Each vent is 2.5 m wide and 2.4 m long except for two vents which are sized, 2.5 m x 1.8 m , 2.5 m x 3.0 m. As seen in the figures, 10 vents were changed in shape and 2 vents remain unchanged. The diagrammatic representation of the install condition of fans and vents is shown in Fig. 5.

The governing equations of numerical analyses are mass conservation equation and Navier-Stokes equations for steady, incompressible flows, described as below:

$$\frac{\partial u_i}{\partial x_i} = 0 \tag{1}$$

$$\frac{\partial(\rho u_j u_i)}{\partial x_j} = -\frac{\partial p}{\partial x_i} + \mu_i \frac{\partial}{\partial x_j}\left(\frac{\partial u_i}{\partial x_j} + \frac{\partial u_j}{\partial x_i}\right) + S_i \tag{2}$$

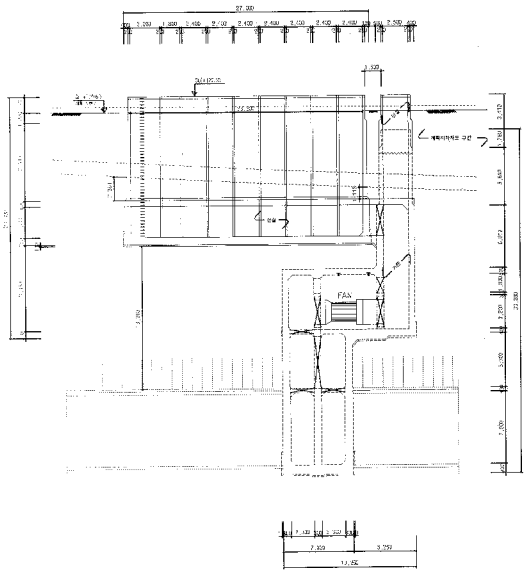

(a) Sectional view

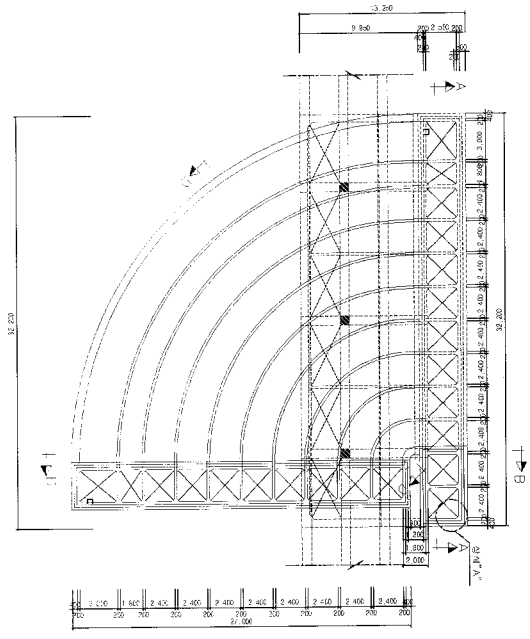

(b) Top view

Fig. 2. A schematic diagram of the vent shaft.

The standard k-ε turbulence model was used for turbulence closure: the model was based on the Boussinesq hypothesis with transport equations for turbulence kinetic energy and its dissipation rate. The equations for turbulence kinetic energy, k and turbulence dissipation rate, ε are given as follows:

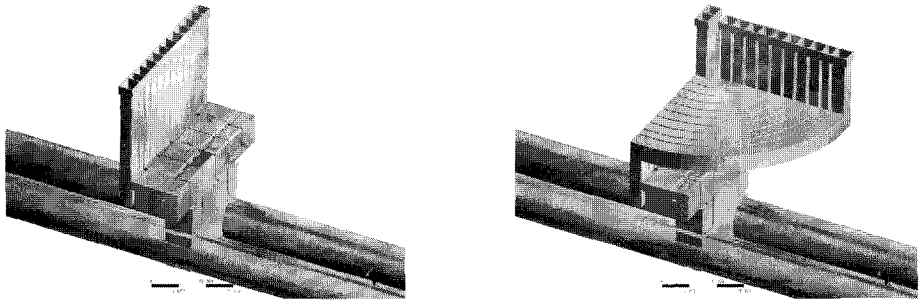

(a) Before construction (b) After construction

Fig. 3. 3D-diagrammatic representation of the vent shaft before and after the shape-change construction.

Fig. 4. Photo of fan in ventilation room.

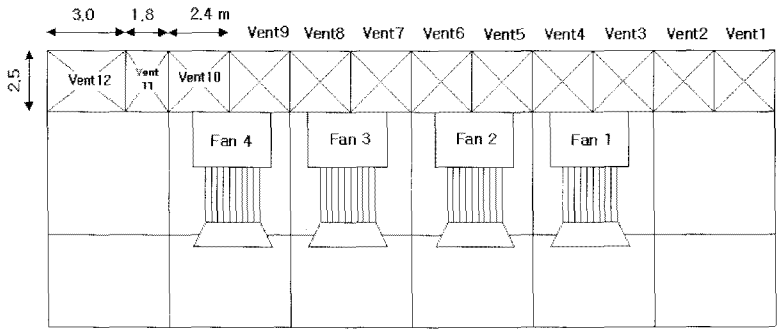

Fig. 5. Diagrammatic representation of the install condition of fans and vents.

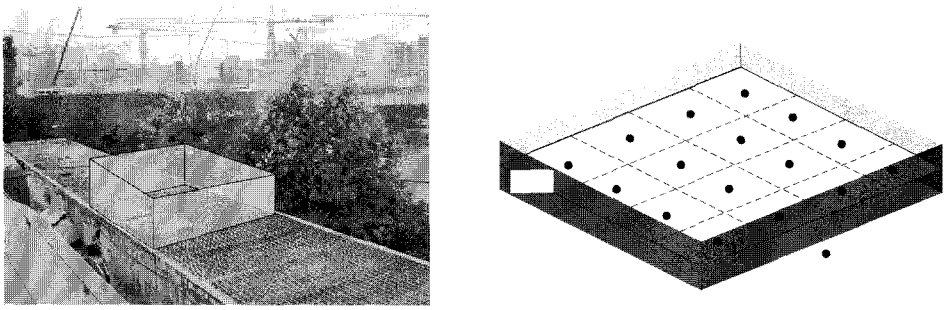

(a) Duct installation for flow rate measurement (b) Grid-centered location of velocity sensor in duct

Fig. 6. A schematic diagram of field experiment.

$$\frac{\partial(\rho u_j k)}{\partial x_j} = \frac{\partial}{\partial x_j}\left((\frac{\mu_t}{\sigma_k})\frac{\partial k}{\partial x_j}\right) + \mu_t\left(\frac{\partial u_i}{\partial x_j} + \frac{\partial u_j}{\partial x_i}\right)\frac{\partial u_i}{\partial x_j} - \rho\varepsilon \quad (3)$$

$$\frac{\partial(\rho u_j \varepsilon)}{\partial x_j} = \frac{\partial}{\partial x_j}\left((\frac{\mu_t}{\sigma_\varepsilon})\frac{\partial \varepsilon}{\partial x_j}\right) + \frac{k}{\varepsilon}\left[C_{\varepsilon 1}\mu_t\left(\frac{\partial u_i}{\partial x_j} + \frac{\partial u_j}{\partial x_i}\right)\frac{\partial u_i}{\partial x_j} - C_{\varepsilon 2}\varepsilon\right] \quad (4)$$

Where $\sigma_k, \sigma_\varepsilon, C_{\varepsilon 1}, C_{\varepsilon 1}$ are constants assigned to standard values of 1.0, 1.3, 1.44 and 1.92, respectively.

The computational models were constructed and solved using CFX11[8], a general purpose commercial CFD software. CFX11 presents the component of Turbomachinery as a solution tool in analyzing the fan-induced flow. Convection terms are discretized using the second-order accurate upwind scheme, while the diffusion terms are discretized using the second order accurate central differencing scheme. The boundary conditions for outlet of tunnel and vent are set as "Opening Condition". The Opening Condition is used in situations where exact details of the flow distribution are unknown but the boundary values of pressure are known. The Opening Condition allows the fluid to cross the domain boundary in either direction, which is decided by ensuring that continuity is satisfied in the computational domain. The rotational effect of fan's impeller was accommodated through the source terms accounting for Coriolis and centrifugal forces. The numerical analyses were conducted to the cases in Table 1.

In this study, field experiments for measuring air flow rate through the vent shaft were carried out to assess the performance of numerical analysis. The duct equipped with 12 sets of velocity sensor was installed on the top of vent shaft as shown in Fig. 6(a). The duct is 2.5 m wide and 2.5 m long, same as vent's dimension and each velocity sensor is located in center of duct grid as shown in Fig. 6(b). The flow rate of one vent was calculated from the velocity and area of each grid according to the guide of flow rate measurement [9]. In experiment, the flow rate of each vent is measured one by one (from vent of No. 1 to No. 12) while the fans remain in operation.

Table 1. Cases of numerical analyses.

CASE	Fan operation condition	Remark
1	Supply(Pull) Operation of fan 1 and fan 3	applied to two different air flow passages of vent shaft ; the condition of before-construction and after-construction
2	Exhaust(Push) Operation of fan 1 and fan 3	
3	Supply(Pull) Operation of fan 2 and fan 4	
4	Exhaust(Push) Operation of fan 2 and fan 4	

3. Results and discussion

Figs. 7 and 8 show the streamlines and velocity distribution around the vent shaft of Case 1 in Table 1. As seen in the figures, the outdoor air is taken into the tunnel through the vent shaft and the fans in vent room. The velocity of air flow in main vents No. 3,4,7,8 that are connected to fan 1 and fan 3 is about 2.5 m/s and some portion of inflow air is induced through other vents.

Fig. 9 shows the mean velocity of each vent of Case 1. The air flow velocity in the main vents for after-construction condition decreased comparing to before-construction condition because of increasing pressure resistance of longer flow passage. On the other hand, in other vents especially No. 1, 2, 5 and 6, the velocity of air for after-construction condition increased comparing to before-construction condition.

Fig. 10 shows the comparison of air flow rate of each vent between the results of the numerical and experimental analyses of Case 3. When evaluating the difference between the experimental and numerical results, it's below 10% except for vents No. 1 and No. 4. Considering the condition of field experiment, the predicted results of numerical analysis show a favorable compatibility with the experimental data.

Fig. 11 shows the air flow rate through each vent under before-construction and after-construction condition quantitatively. While the results of Case 1 is shown in Fig. 11(a), the air flow rate through the main vents No. 3, 4, 7, 8 for fan 1 and fan 3 decreased by 9.7% to 23.3% , resulting from the change to vent shaft. Especially for vent No. 7 and 8 in which the length of air flow passage increased significantly, the drop of air flow rate were 17.5% and 23.3%, respectively. On the other hand, in other vents especially No. 1, 2, 5 and 6, the air flow rate for after-construction condition increased from before-construction condition. Such cause can be explained as; while the main vents and other vents are connected in base part, the rise of pressure resistance in main vents caused the

supply air to flow through other vents more than before-construction condition. So, with 5,893 CMM of the supply air flow for before-construction condition and 5,765 CMM for after-construction condition, the overall flow rate through the vent shaft after shape-change construction decreased by about 2.2%.

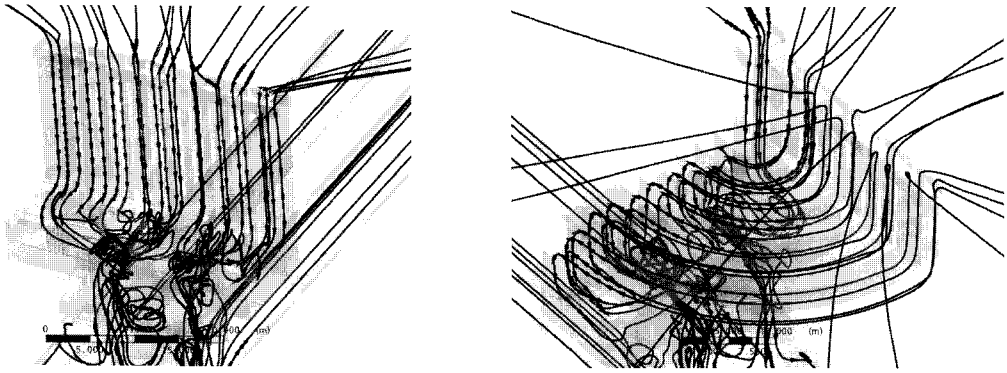

(a) Before construction (b) After construction

Fig. 7. Streamlines around the vent shaft of Case 1.

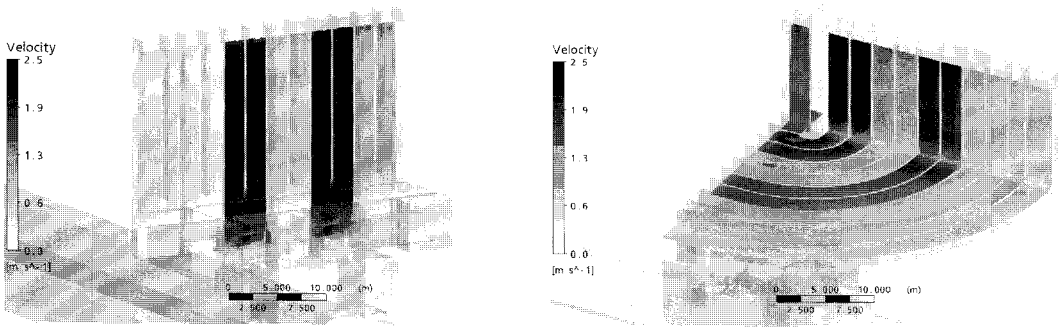

(a) Before construction (b) After construction

Fig. 8. Velocity distributions around the vent shaft of Case 1.

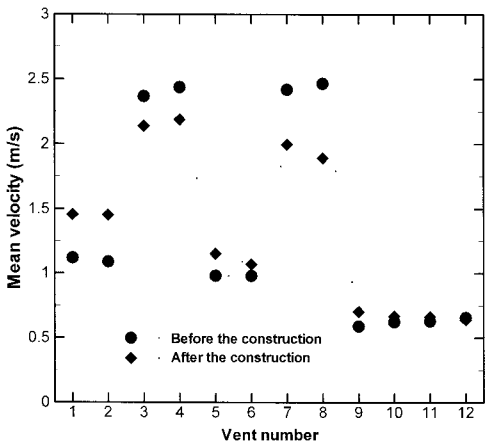

Fig. 9. Mean velocity in each vent of Case 1.

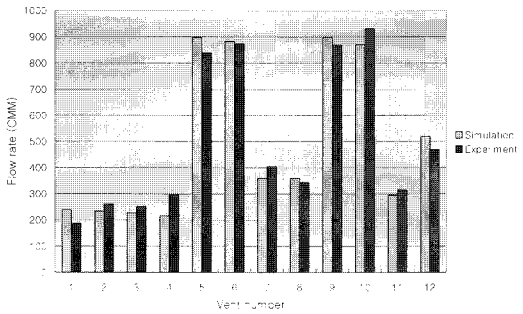

Fig. 10. Comparison of flow rate through each vent between experimental and numerical result of Case 3.

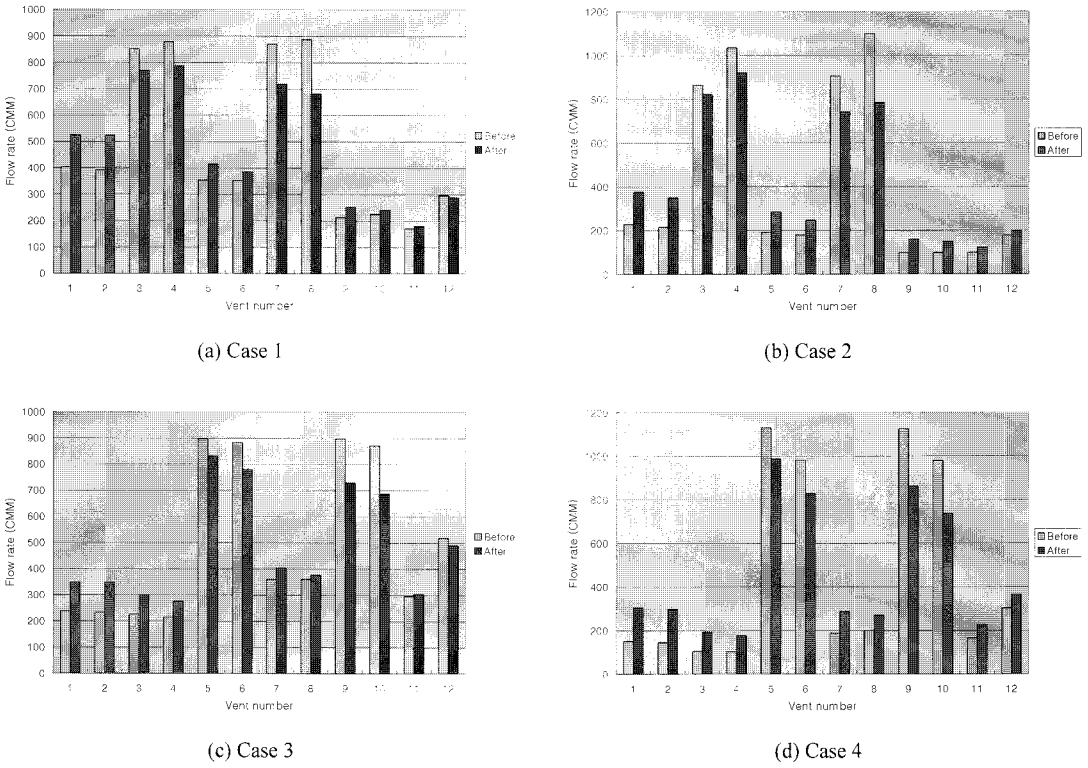

(a) Case 1

(b) Case 2

(c) Case 3

(d) Case 4

Fig. 11. Comparison of flow rate through each vent between before-construction and after-construction condition.

As a result of Case 2 in Fig. 11(b), the exhaust air flow rate through vent No. 3, No. 4, No. 7, No. 8 decreased by 4.9%, 11.1%, 18.1%, 28.7% , respectively. But like Case1, flow rate of other vents increased 65.1% for vent No. 1, 63.0% for No. 2 and so forth. The Fig. 11(c) and Fig. 11(d) show the results of Case 3 and Case 4 in which the main vent No. 5, No. 6, No. 9 and No. 10 are connected to fan 2 and fan 4. The tendency to change of air flow rate of Case 3 and Case 4 is similar with the Case 1 and Case 2.

Table 2 shows the overall flow rate through the vent shaft and the reduction ratio of air flow for

Table 2. Variations of the overall flow rate through the vent shaft between before-construction and after-construction conditions of each case.

Case	Overall flow rate (CMM)		Reduction ratio of flow rate (%)
	Before	After	
1	5,893	5,765	2.2
2	5,185	5,148	0.7
3	5,995	5,872	2.1
4	5,574	5,525	0.9

before-construction and after-construction condition in each case. The decreases of air flow rate due to vent-shaft change were between 0.7 to 2.2% in the cases examined

4. Conclusion

A three-dimensional numerical analysis of mechanical ventilation system in vent shaft of the subway in operation was carried out in association with the different air flow passage of vent shaft and two push/pull ventilation operation modes. The ventilation characteristics of vent shaft in relation with the shape change were evaluated. As a result, the following conclusion was made.

(1) While the differences of air flow rate in each vent between the experimental and numerical results are below 10 % excepts for 2 vents, the predicted results of numerical analysis show a favorable compatibility with the experimental data.
(2) The velocity of air flow taken into the main vents that are connected to the fans in operation in Case 1 was about 2.5 m/s and some portion of incoming air was induced through other vents.
(3) The air flow rate in main vents at after-construction condition decreased comparing to before-construction condition due to increasing pressure resistance of longer flow passage, but the air flow rate of other vents increased.
(4) While the main vents and other vents are connected in base part, the rise of pressure resistance in main vents caused the supply air to flow through other vents more than before-construction condition. Therefore, after the shape-change construction the air flow is redistributed towards reducing the flow rate variation between the main vents and the other vents.
(5) The decreases of overall air flow rate due to vent-shaft change were between 0.7 to 2.2% in the cases examined

References

[1] USDT (United States Department of Transportation) 1976 *Subway Environmental Design Handbook.*
[2] Hara, T. 1967 Aerodynamic drag of trains in tunnels. Quarterly Report of Railway Technical Research Institute, Vol.8, No.4, pp.229-235.
[3] Saiben, M. 1971 Fluid mechanics of train-tunnel systems in unsteady motion. AIAA Journal, Vol.9, No.8, pp.1538-1545.
[4] Institute for Rapid Transit 1972 *Subway Aerodynamic and Thermodynamic Test (SAT) Facility Single-Track Aerodynamics.* Technical Report No. UMTA-DC-MTD-7-72-15.
[5] Kim, J.Y. & Kim, K.Y. 2007 Experimental and numerical analysis of train-induced unsteady tunnel flow in subway. Tunneling and Underground Space Technology, Vol.22, pp166-172.
[6] Yau, R., Cheng, V., Lau, K.P. & Lai, F. 2003 Design and analysis of tunnel ventilation system for the extension of an existing railway tunnel in Hong Kong. 11th International Symposium on the Aerodynamics & Ventilation of Vehicle Tunnel, Luzern Switzerland, pp.323-337.
[7] Mckinney, D.M. & Miclea, P.C. 2003 Use of CFD to estimate airflow through PSDs during train dwell. 11th International Symposium on the Aerodynamics & Ventilation of Vehicle Tunnel, Luzern Switzerland, pp.631-641.
[8] CFX 11 2007 *CFX11 Documentation*, Ansys Inc.
[9] SAREK 2001 *Handbook of Air-Conditioning and Refrigeration* [Korean]